

## Accepted Manuscript

Synthesis and evaluation of  $\text{Re}^{99\text{mTc}}(\text{I})$  complexes bearing a somatostatin receptor-targeting antagonist and labeled via a novel [N,S,O] clickable bifunctional chelating agent

Lauren L. Radford, Dionysia Papagiannopoulou, Fabio Gallazzi, Ashley Berendzen, Lisa Watkinson, Terry Carmack, Michael R. Lewis, Silvia S. Jurisson, Heather M. Hennkens

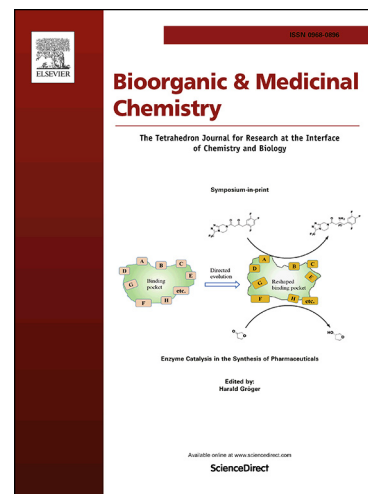
PII: S0968-0896(18)31627-4  
DOI: <https://doi.org/10.1016/j.bmc.2018.12.028>  
Reference: BMC 14677

To appear in: *Bioorganic & Medicinal Chemistry*

Received Date: 23 September 2018  
Revised Date: 11 December 2018  
Accepted Date: 20 December 2018

Please cite this article as: Radford, L.L., Papagiannopoulou, D., Gallazzi, F., Berendzen, A., Watkinson, L., Carmack, T., Lewis, M.R., Jurisson, S.S., Hennkens, H.M., Synthesis and evaluation of  $\text{Re}^{99\text{mTc}}(\text{I})$  complexes bearing a somatostatin receptor-targeting antagonist and labeled via a novel [N,S,O] clickable bifunctional chelating agent, *Bioorganic & Medicinal Chemistry* (2018), doi: <https://doi.org/10.1016/j.bmc.2018.12.028>

This is a PDF file of an unedited manuscript that has been accepted for publication. As a service to our customers we are providing this early version of the manuscript. The manuscript will undergo copyediting, typesetting, and review of the resulting proof before it is published in its final form. Please note that during the production process errors may be discovered which could affect the content, and all legal disclaimers that apply to the journal pertain.



Synthesis and evaluation of Re/<sup>99m</sup>Tc(I) complexes bearing a somatostatin receptor-targeting antagonist and labeled via a novel [N,S,O] clickable bifunctional chelating agent

Lauren L. Radford<sup>a</sup>, Dionysia Papagiannopoulou<sup>b</sup>, Fabio Gallazzi<sup>a,c</sup>, Ashley Berendzen<sup>d</sup>, Lisa Watkinson<sup>d</sup>, Terry Carmack<sup>d</sup>, Michael R. Lewis<sup>d,e</sup>, Silvia S. Jurisson<sup>a</sup>, Heather M. Hennkens<sup>a,f,\*</sup>

<sup>a</sup>Department of Chemistry, University of Missouri, 601 S. College Ave. Columbia, Missouri 65211, USA

<sup>b</sup>School of Pharmacy, Aristotle University of Thessaloniki, 54124, Thessaloniki, Greece

<sup>c</sup>Molecular Interaction Core, University of Missouri, 601 S. College Ave. Columbia, Missouri 65211, USA

<sup>d</sup>Research Service, Harry S. Truman Memorial Veterans' Hospital, 800 Hospital Dr. Columbia, Missouri 65212, USA

<sup>e</sup>Department of Veterinary Medicine and Surgery, University of Missouri, 900 E Campus Dr. Columbia, Missouri 65211, USA

<sup>f</sup>University of Missouri Research Reactor Center, 1513 Research Park Dr. Columbia, Missouri 65211, USA

\*Corresponding author:

Tel: + 1 573 882 5355

Fax: +1 573 882 6360

Email: [HennkensH@missouri.edu](mailto:HennkensH@missouri.edu)

List of abbreviations

**DIEA** N,N-diisopropylethylamine

**GA** gentisic acid

**HRMS** high resolution mass spectrometry

**ICP-MS** inductively coupled plasma mass spectrometry

**LC-ESI-MS** liquid chromatography electrospray ionization mass spectrometry

**NET** neuroendocrine tumor

**PBS** phosphate buffered saline

**RCY** radiochemical yield

**SPECT** single-photon emission computed tomography

**SPPS** solid-phase peptide synthesis

**SSTR** somatostatin receptor

**SSTR2** somatostatin receptor subtype 2

Keywords

rhenium; technetium-99m; tricarbonyl; bifunctional chelator; click chemistry; somatostatin receptor antagonists; biodistribution; imaging

Abstract

The somatostatin receptor subtype 2 (SSTR2) is often highly expressed on neuroendocrine tumors (NETs), making it a popular *in vivo* target for diagnostic and therapeutic approaches aimed toward management of NETs. In this work, an antagonist peptide (sst<sub>2</sub>-ANT) with high affinity for SSTR2 was modified at the *N*-terminus with a novel [N,S,O] bifunctional chelator (**2**) designed for tridentate chelation of rhenium(I) and technetium(I) tricarbonyl cores, [Re(CO)<sub>3</sub>]<sup>+</sup> and [<sup>99m</sup>Tc][Tc(CO)<sub>3</sub>]<sup>+</sup>. The chelator-peptide conjugation was performed via a Cu(I)-assisted click reaction of the alkyne-bearing chelator (**2**) with an azide-functionalized sst<sub>2</sub>-ANT peptide (**3**), to yield NSO-sst<sub>2</sub>-ANT (**4**). Two synthetic methods were used to prepare Re-**4** at the macroscopic scale, which differed based on the relative timing of the click conjugation to the [Re(CO)<sub>3</sub>]<sup>+</sup> complexation by **2**. The resulting products demonstrated the expected molecular mass and nanomolar *in vitro* SSTR2 affinity (IC<sub>50</sub> values under 30 nM, AR42J cells, [<sup>125</sup>I]iodo-

Tyr<sup>11</sup>-somatostatin-14 radioligand standard). However, a difference in their HPLC retention times suggested a difference in metal coordination modes, which was attributed to a competing N-triazole donor ligand formed during click conjugation. Surprisingly, the radiotracer scale reaction of [<sup>99m</sup>Tc][Tc(OH<sub>2</sub>)<sub>3</sub>(CO)<sub>3</sub>]<sup>+</sup> (<sup>99m</sup>Tc; t<sub>1/2</sub> = 6 h, 141 keV γ) with **4** formed a third product, distinct from the Re analogues, making this one of the unusual cases in which Re and Tc chemistries are not well matched. Nevertheless, the [<sup>99m</sup>Tc]Tc-**4** product demonstrated excellent *in vitro* stability to challenges by cysteine and histidine (≥98% intact through 24 h), along with 75% stability in mouse serum through 4 h. *In vivo* biodistribution and microSPECT/CT imaging studies performed in AR42J tumor-bearing mice revealed improved clearance of this radiotracer in comparison to a similar [<sup>99m</sup>Tc][Tc(CO)<sub>3</sub>]-labeled sst<sub>2</sub>-ANT derivative previously studied. Yet despite having adequate tumor uptake at 1 h (4.9% ID/g), tumor uptake was not blocked by co-administration of a receptor-saturating dose of SS-14. Aimed toward realignment of the Re and Tc product structures, future efforts should include distancing the alkyne group from the intended donor atoms of the chelator, to reduce the coordination options available to the [M(CO)<sub>3</sub>]<sup>+</sup> core (M = Re, <sup>99m</sup>Tc) by disfavoring involvement of the N-triazole.

## 1 Introduction

Several clinical imaging agents are currently available for detecting neuroendocrine tumors (NETs) by targeting of somatostatin receptors (SSTRs) using radiolabeled octreotide derivatives, such as [<sup>68</sup>Ga]Ga-DOTA-Tyr<sup>3</sup>-octreotate (NETSPOT<sup>TM</sup>) and [<sup>111</sup>In]In-DTPA-octreotide (Octreoscan<sup>TM</sup>). Of the FDA-approved NET radiopharmaceuticals available in the United States, none use <sup>99m</sup>Tc (<sup>99m</sup>Tc-Tektrotyd is approved in Europe) and all of them act as SSTR agonists. There is now a rapidly-growing initiative to investigate the properties of radiolabeled antagonist

peptides due to their ability to bind selectively, and with high affinity, to *in vivo* targets that have traditionally been targeted using agonist peptides.<sup>1-7</sup> In this work, the antagonist peptide 4-NO<sub>2</sub>-Phe-c(DCys-Tyr-DTrp-Lys-Thr-Cys)-DTyr-NH<sub>2</sub> (sst<sub>2</sub>-ANT) was used as the targeting vector due to its high affinity for somatostatin receptor subtype 2 (SSTR2),<sup>1</sup> which is the most frequently overexpressed of the five SSTR subtypes found on NETs.<sup>8,9</sup> Additionally, the antagonist [<sup>111</sup>In]In-DOTA-sst<sub>2</sub>-ANT was demonstrated to label a higher number of SSTR2 binding sites than a similar agonist peptide, [<sup>111</sup>In]In-DTPA-Tyr<sup>3</sup>-octreotate.<sup>1</sup> And in a small clinical trial, [<sup>111</sup>In]In-DOTA-sst<sub>2</sub>-ANT outperformed Octreoscan™ by locating a higher number of NET metastases,<sup>10</sup> further demonstrating the potential of this SSTR-targeting sequence. Very little work has been performed using SSTR-targeting antagonist peptides labeled with <sup>99m</sup>Tc, a widely available and inexpensive radioisotope that is well established in nuclear medicine clinics worldwide. The decay properties of <sup>99m</sup>Tc (t<sub>1/2</sub> = 6 h) are greatly advantageous for imaging using single-photon emission computed tomography (SPECT), particularly its high abundance gamma emission (141 keV, 89%). Development of a <sup>99m</sup>Tc-labeled SSTR2-targeting radiopharmaceutical could provide an additional diagnostic tool for imaging NETs that would be more accessible to a larger percentage of the patient population and thus help lessen medical disparities.

We recently reported on the chelation of the tricarbonylrhenium (I) and [<sup>99m</sup>Tc]tricarbonyltechnetium (I) cations via an [N,S,N] bifunctional chelator (Figure 1A) that was conjugated to sst<sub>2</sub>-ANT.<sup>11,12</sup> The resulting [<sup>99m</sup>Tc][Tc(CO)<sub>3</sub>]-labeled, monocationic complex successfully targeted SSTR2s in a tumor-bearing mouse model, but exhibited slow hepatobiliary and renal clearance that diminished its potential as an imaging agent. Several factors can affect the *in vivo* behavior of a radiometallated bioconjugate, including the bifunctional chelator,<sup>13</sup> the

linker,<sup>14,15</sup> the metal,<sup>16</sup> and the overall charge.<sup>17-19</sup> We aimed here to improve the pharmacokinetic properties of [<sup>99m</sup>Tc][Tc(CO)<sub>3</sub>]-labeled sst<sub>2</sub>-ANT by using a new tridentate [N,S,O] bifunctional chelator. An [N,S,O] chelator designed to form neutral metal tricarbonyl complexes may help reduce the charge impact the metal-chelator complex has on the peptide's *in vivo* behavior.<sup>17,20</sup> Additionally, [N,S,O] donor systems are preferred over certain [N,S,N] systems by the [M(CO)<sub>3</sub>]<sup>+</sup> core (M = Re, <sup>99m</sup>Tc). For example, Karagiorgou et al. demonstrated that in the presence of four possible donor atoms (N-primary amine, S-thioether, N-pyridine amine, and O-carboxylate), both <sup>99m</sup>Tc and Re tricarbonyl cores preferentially bound via the [N,S,O] binding mode over the expected [N,S,N<sub>pyr</sub>] mode, despite the occurrence of a larger 7-membered ring in the former.<sup>21</sup> Herein, we report the synthesis of a novel [N,S,O] bifunctional chelator for the [M(CO)<sub>3</sub>]<sup>+</sup> organometallic core (**2**, Figure 1B) along with its bioconjugation to the sst<sub>2</sub>-ANT peptide using click chemistry to yield NSO-sst<sub>2</sub>-ANT (**4**). Additionally, we describe the synthesis of the Re-**4** and [<sup>99m</sup>Tc]Tc-**4** complexes and their *in vitro* and *in vivo* evaluations as potential SSTR-targeting agents.

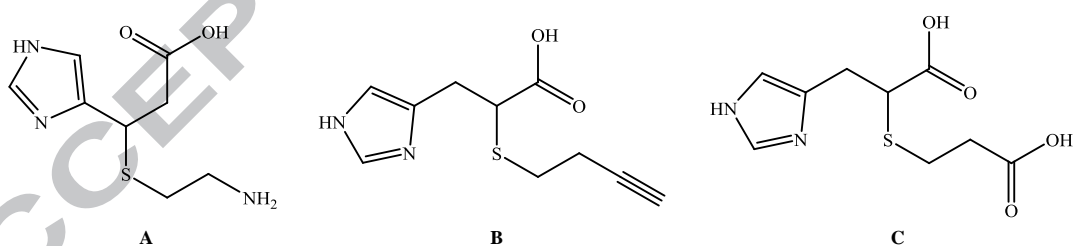


Figure 1. Structures of (A) the previously studied [N,S,N] chelator,<sup>12</sup> (B) the current [N,S,O] chelator, **2**, and (C) the previously studied [N,S,O] chelator.<sup>25</sup>

## 2 Methods and Materials

### 2.1 General Methods and Instrumentation

All chemicals were reagent grade from Sigma-Aldrich, unless otherwise specified, and used as received. [<sup>125</sup>I]Iodo-Tyr<sup>11</sup>-somatostatin-14 was purchased from Perkin Elmer (Waltham, MA). All solvents used for high performance liquid chromatography (HPLC) were HPLC-grade and were passed through 0.22 μm membrane filters prior to use. For HPLC mobile phase and radiotracer experiments, purified 18 MΩ.cm water (Thermo Barnstead) was used unless otherwise stated. Solid-phase peptide synthesis (SPPS) was performed on an Apex 396 peptide synthesizer from AAPPTec (Louisville, KY). All reagents for peptide synthesis were purchased from AAPPTec, Chem-Impex International, Inc. (Wood Dale, IL), and Oakwood Chemicals (West Columbia, SC).

Three HPLC systems were used. System 1 was used for semi-preparative HPLC separations and liquid chromatography electrospray ionization mass spectrometry (LC-ESI-MS) analyses. This HPLC system was comprised of a Beckmann Coulter Gold HPLC equipped with a 168 diode array detector and 507e auto-injector and was coupled to an ion trap mass analyzer (LCQ FLEET instrument with positive ion ionization; Thermo Fisher Scientific, Waltham, MA). Semi-preparative purifications were performed on a Waters Nova-Pak C18 preparative column (300 mm x 19 mm x 6 μm, 60 Å) using a linear gradient of 20% to 50% acetonitrile (MeCN) with 0.1% trifluoroacetic acid (TFA) (solvent A) in H<sub>2</sub>O with 0.1% TFA (solvent B) over 60 min with a flow rate of up to 10 mL/min (Method 1) and UV detection at 280 nm and either 225 or 235 nm. LC-ESI-MS analyses used a Thermo Scientific BetaBasic C18 analytical column (150 mm x 4.6 mm x 5 μm, 150 Å) and a linear gradient of 10% to 50% solvent A in solvent B over 30 min (Method 2) with a flow rate of 1 mL/min and UV detection at 214 nm, 254 nm and/or

280 nm. The HPLC was controlled using the 32 KARAT software package (Beckmann Coulter, Fullerton, CA) and MS data were analyzed using Thermo Fisher Scientific XCalibur software.

System 2 was an Agilent HP 1100 series pump connected to an HP 1100 multiple wavelength detector. A semi-preparative Agilent Eclipse XDB-C18 column (250 mm x 9.4 mm x 5  $\mu\text{m}$ , 80  $\text{\AA}$ ) was used with a linear gradient of 0% to 75% MeOH (solvent C) in solvent B over 15 min (Method 3) with a flow rate of 2 mL/min and UV detection at 254 nm.

System 3 was a Shimadzu Prominence HPLC with an SPD-20AV multiple wavelength detector connected in-line to a NaI(Tl) detector, which also used a Thermo Scientific BetaBasic reversed-phase C18 column (150 mm x 4.6 mm x 5  $\mu\text{m}$ , 150  $\text{\AA}$ ). The linear gradient was 28% to 36% solvent A in solvent B over 20 min (Method 4). The flow rate was 1 mL/min with UV detection at 254 and 280 nm.

NMR analyses were performed using an Agilent DD2 500 MHz spectrometer (Agilent, Santa Clara, CA) or a Bruker Avance III 500 MHz spectrometer (Bruker, Billerica, MA). Inductively coupled plasma mass spectrometry (ICP-MS) analyses were performed on a VG Axiom SC high-resolution ICP-MS (Thermo Fisher, Waltham, MA). High resolution mass spectrometry (HRMS) analyses were performed on a Perseptive Biosystems Mariner atmospheric pressure ionization time-of-flight instrument (API-Tof) operated in positive mode. The sample was introduced into an electrospray ionization source using a 1:1 mixture of MeCN/H<sub>2</sub>O. The mass was externally calibrated to CsI adducts.

## 2.2 Synthesis of but-3-yn-1-yl methanesulfonate (1a)

Into a 100 mL round bottom flask containing 40 mL of anhydrous dichloromethane (DCM), 790  $\mu\text{L}$  of 3-butynol (10 mmol) and 2.8 mL of triethylamine (20 mmol) were added. The reaction

mixture was brought to  $-10\text{ }^{\circ}\text{C}$  using a salty ice bath. A pressure-equalizing addition funnel containing  $850\text{ }\mu\text{L}$  of methane sulfonyl chloride (MsCl,  $11\text{ mmol}$ ) in  $10\text{ mL}$  of anhydrous DCM was placed on the flask, the entire apparatus was flushed with  $\text{N}_2$  gas, and a light  $\text{N}_2$  gas flow was maintained for the duration of the reaction. Over a period of  $25\text{ min}$ , the MsCl solution was added to the round bottom flask. The reaction was allowed to continue at  $-10\text{ }^{\circ}\text{C}$  for  $1\text{ h}$  and then at room temperature for an additional  $1.5\text{ h}$ . The reaction mixture was washed three times with equal parts water, and the organic layer was dried over  $\text{MgSO}_4$  and then filtered. Removal of the solvent yielded a light yellow oil ( $1.37\text{ g}$ ) in  $90\%$  yield. The product was characterized by NMR. Observed shifts were similar to those previously reported for the product (prepared via a similar synthetic route).<sup>22</sup>  $^1\text{H}$  NMR ( $300\text{ MHz}$ ,  $\text{CDCl}_3$ )  $\delta$ :  $4.32$  (t,  $2\text{H}$ ),  $3.06$  (s,  $3\text{H}$ ),  $2.68$  (t,  $2\text{H}$ ),  $2.08$  (s,  $1\text{H}$ ).  $^{13}\text{C}$  NMR ( $75\text{ MHz}$ ,  $\text{CDCl}_3$ )  $\delta$ :  $78.59$ ,  $70.79$ ,  $66.95$ ,  $37.67$ ,  $19.72$ .

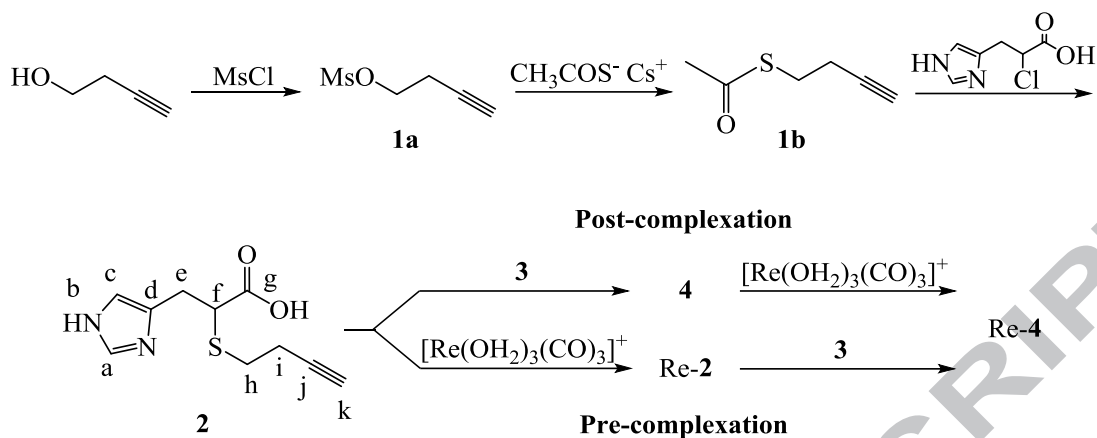
### 2.3 Synthesis of S-(but-3-yn-1-yl) ethanethioate (**1b**)

A  $250\text{ mL}$ , three-neck round bottom flask was fitted with a reflux condenser, a pressure-equalizing addition funnel, and a glass stopper. The entire apparatus was purged with  $\text{N}_2$  gas, and a gentle flow was then maintained for the duration of the reaction. In the flask,  $2.0\text{ mg}$  of  $\text{Cs}_2\text{CO}_3$  ( $6.1\text{ mmol}$ ) was suspended in  $125\text{ mL}$  of anhydrous MeCN and then, directly to this,  $544\text{ }\mu\text{L}$  of thioacetic acid ( $7.3\text{ mmol}$ ) was added, which caused the suspension to become slightly yellow. The reaction was held at  $50\text{ }^{\circ}\text{C}$  for  $30\text{ min}$ , after which time a solution containing  $903\text{ mg}$  of **1a** ( $6.1\text{ mmol}$ ) in  $25\text{ mL}$  anhydrous MeCN was added dropwise via the addition funnel, and the reaction was continued for  $7\text{ h}$  at  $55\text{ }^{\circ}\text{C}$ . The reaction mixture was filtered to remove solids and then concentrated via rotary evaporation to yield a volatile oil ( $0.7\text{ g}$ ) in  $82\%$  yield. Observed NMR shifts were similar to those previously reported for the product (prepared via a similar

synthetic route).<sup>22</sup> <sup>1</sup>H NMR (300 MHz, CDCl<sub>3</sub>) δ: 3.07-2.99 (m, 2H), 2.52-2.42 (m, 2H), 2.34 (s, CH<sub>3</sub>, 3H), 2.03-1.98 (m, 1H). <sup>13</sup>C NMR (75 MHz, CDCl<sub>3</sub>) δ: 194.90 (CO), 81.97, 69.55, 30.43, 28.09 (CH<sub>3</sub>), 19.44.

#### 2.4 Synthesis of 2-(but-3-yn-1-ylthio)-3-(1H-imidazol-4-yl)propanoic acid (2)

Into a 100 mL round bottom flask, 292 mg of **1b** (2.3 mmol) was dissolved in 2.7 mL of 1 M NaOH (2.7 mmol). The flask was then sealed with a rubber septum and flushed with N<sub>2</sub> gas for 1.5 h. A solution of 397 mg of 2-chloro-3-(1H-imidazol-4-yl)propanoic acid (2.3 mmol) in 3 mL H<sub>2</sub>O was added dropwise via a syringe, followed by 2.7 mL of 2 M NaOH for a final concentration of 1 M NaOH (8.1 mmol). The reaction was stirred at room temperature for 7 days. The pH of the solution was adjusted to 7 with 3.8 mL of 1 M HCl, and the solvent was evaporated to dryness. To the residue, 40 mL of an EtOH:H<sub>2</sub>O mixture (3:1) was added. The brown solids were filtered, and the filtrate was evaporated to dryness. The dry residue (420 mg) was dissolved in 1 mL of H<sub>2</sub>O:MeOH (95:5) and processed in batches by loading onto a Sep-Pak Vac C-18 cartridge and elution with ~20 mL of H<sub>2</sub>O:MeOH (95:5). The combined yield was 140 mg of purified **2** (colorless oil, 27% yield). NMR assignments (Scheme 1) were made using HSQC. <sup>1</sup>H NMR (500 MHz, D<sub>2</sub>O) δ: 8.42 (s, 1H, a), 7.13 (s, 1H, c), 3.46 (dd, J = 7.8, 7.2 Hz, 1H, f), 3.05 (dd, J = 15.4, 8.1 Hz, 1H, e), 2.93 (dd, J = 15.3, 7.0 Hz, 1H, e), 2.62 (tt, J = 13.3, 6.6 Hz, 2H, h), 2.36 (dd, J = 8.1, 5.7 Hz, 2H, i), 2.24 (s, 1H, k). <sup>13</sup>C NMR (75 MHz, CD<sub>3</sub>OD) δ: 177.95 (g), 134.04 (a), 133.73 (d), 117.76 (c), 82.30 (j), 69.08 (k), 50.24 (f), 30.28 (e), 29.78 (h), 19.21 (i). HRMS (*m/z*): (C<sub>10</sub>H<sub>12</sub>N<sub>2</sub>O<sub>2</sub>S) 225.0692 calc. for [M+H]<sup>+</sup>, 225.0849 found and 449.1312 calc. for [2M+H]<sup>+</sup>, 449.1440 found.



Scheme 1. General reaction scheme illustrating the synthesis of **2** and the subsequent pre- and post-complexation methods used to synthesize Re-**4**.

2.5 Syntheses of  $\text{N}_3\text{CH}_2\text{CO}-4\text{NO}_2\text{-Phe-c}(\text{D}\text{Cys-Tyr-D}\text{Trp-Lys-Thr-Cys})\text{-D}\text{Tyr-NH}_2$  ( $\text{N}_3\text{-sst}_2\text{-ANT}$ , **3**) and  $2\text{-}4\text{NO}_2\text{-Phe-c}(\text{D}\text{Cys-Tyr-D}\text{Trp-Lys-Thr-Cys})\text{-D}\text{Tyr-NH}_2$  ( $\text{NSO-sst}_2\text{-ANT}$ , **4**)

The antagonist peptide, sst<sub>2</sub>-ANT, was synthesized using conventional 9-fluorenylmethoxycarbonyl (Fmoc) SPPS using Sieber amide resin.<sup>12</sup> The peptide was azido-derivatized at the *N*-terminus by adding 2-azidoacetic acid via an amide linkage as the final elongation step. The azidoacetyl-functionalized peptide (**3**, in linear form) was then click conjugated to **2** via a Cu(I)-assisted azide-alkyne cycloaddition reaction to yield **4** (Figure 2B). Here, the protected and resin-bound peptide was placed in a 1:1 dimethylformamide (DMF):tetrahydrofuran (THF) solution containing two equivalents of CuI and 30 equivalents of *N,N*-diisopropylethylamine (DIEA). To this solution, two equivalents of **2** in 1:1 DMF:THF were added. The reaction mixture was allowed to stir overnight at room temperature before being deprotected and cleaved from the resin using a solution of 87.5% TFA, 2.5% thioanisole, 2.5% phenol, 2.5% water, 2.5% ethanedithiol and 2.5% triisopropylsilane. LC-ESI-MS analysis of the crude product demonstrated that disulfide cyclization had also occurred, thus no additional cyclization step was required. Semi-preparative HPLC purification (System 1, Method 1) was

used to collect pure fractions of both **4** and the unconjugated, cyclized **3** that remained (Figure 2A). The purified fractions were combined, lyophilized and stored at -20 °C. HRMS ( $m/z$ ): **3** ( $C_{56}H_{67}N_{15}O_{14}S_2$ ) 1238.4506 calc. for  $[M+H]^+$ , 1238.4533 found; **4** ( $C_{66}H_{79}N_{17}O_{16}S_3$ ) 1462.5126 calc. for  $[M+H]^+$ , 1462.5363 found and 731.7599 calc. for  $[M+2H]^{2+}$ , 731.7752 found.  $t_R$ : 23.3 min for **3** and 18.0 min for **4** (System 1, Method 2).

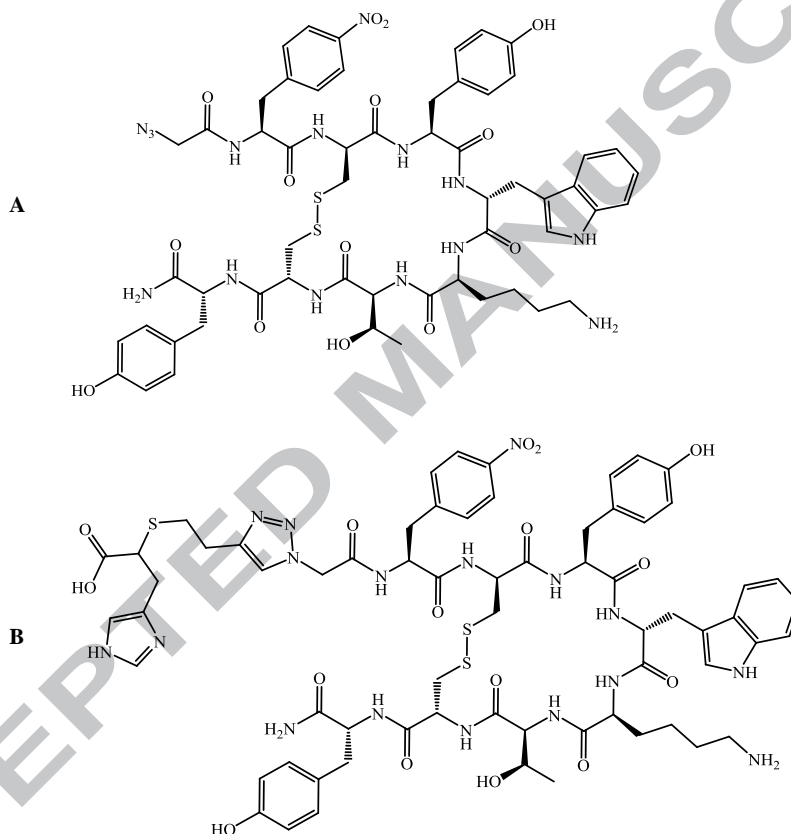


Figure 2. Structures of (A) the azide-functionalized  $sst_2$ -ANT peptide, **3**, and (B) the NSO- $sst_2$ -ANT chelator-peptide bioconjugate, **4**.

## 2.6 Post-complexation Synthesis of *fac*-[Re(CO)<sub>3</sub>(**4**)] (Re-**4**-post)

In the post-complexation method, the chelator was labeled with the tricarbonyl metal core following click conjugation to the peptide (Scheme 1). A solution of  $[Re(OH_2)_3(CO)_3]^+$  was

prepared by dissolving  $(\text{NEt}_4)_2[\text{Re}(\text{CO})_3\text{Br}_3]$  (13.8 mg, 0.018 mmol) in 500  $\mu\text{L}$  of  $\text{H}_2\text{O}$ , adding  $\text{AgNO}_3$  (10.1 mg, 0.06 mmol), and stirring at room temperature for 15 min before filtering off the precipitate.<sup>23</sup> The precipitate was washed with an additional 500  $\mu\text{L}$  of  $\text{H}_2\text{O}$  to yield a filtrate with a final volume of 1 mL and 18 mM  $[\text{Re}(\text{OH}_2)_3(\text{CO})_3]^+$ . In a 1.5 mL centrifuge tube, 1.9 mg (0.0013 mmol) of purified **4** was dissolved in 190  $\mu\text{L}$  of 20% MeOH (aq) and 110  $\mu\text{L}$  of the  $[\text{Re}(\text{OH}_2)_3(\text{CO})_3]^+$  solution (0.002 mmol). The vial was then heated for 3 h at 55 °C in an Eppendorf Thermomixer C (Eppendorf, Hauppauge, NY) fitted with a heating block for 1.5 mL tubes. The reaction was monitored using HPLC, which showed production of two isomers in a ~1:1 ratio with a yield of 84%. The Re-**4-post** isomers were purified collectively using analytical HPLC, and fractions of high purity were combined, lyophilized, and stored at -20 °C. HRMS ( $m/z$ ):  $(\text{C}_{69}\text{H}_{78}\text{N}_{17}\text{O}_{19}^{187}\text{ReS}_3)$  1732.4453 calc. for  $[\text{M}+\text{H}]^+$ , 1732.5758 found and 866.7263 calc. for  $[\text{M}+2\text{H}]^{2+}$ , 866.7838 found.  $t_{\text{R}}$ : 9.8 and 10.2 min (System 3, Method 4).

### 2.7 Pre-complexation Synthesis of *fac*- $[\text{Re}(\text{CO})_3(\mathbf{4})]$ (Re-**4-pre**)

In the pre-complexation labeling method, the chelator was labeled with the tricarbonyl metal core prior to click conjugation to the peptide (Scheme 1). A solution of  $[\text{Re}(\text{OH}_2)_3(\text{CO})_3]^+$  was prepared as described above using 38 mg of  $(\text{NEt}_4)_2[\text{Re}(\text{CO})_3\text{Br}_3]$  (0.05 mmol) in 2 mL of  $\text{H}_2\text{O}$  and 25 mg of  $\text{AgNO}_3$  (0.15 mmol). To this solution, 11 mg of **2** (0.05 mmol) and 5 mg of  $\text{NaHCO}_3$  (0.05 mmol) were added. After heating the reaction at 65 °C for 2 h, the solvent was evaporated to dryness and THF was added to the residue. The solids formed were filtered off, and the filtrate was concentrated to dryness. The crude product (25 mg) was purified by semi-preparative HPLC (System 2, Method 3), yielding 18 mg (after drying) of *fac*- $[\text{Re}(\text{CO})_3(\mathbf{2})]$  (Re-**2**) as an off-white solid (yield: 73%). IR (KBr,  $\text{cm}^{-1}$ ): 2031, 1910, 1636.  $^1\text{H}$  NMR (500 MHz,

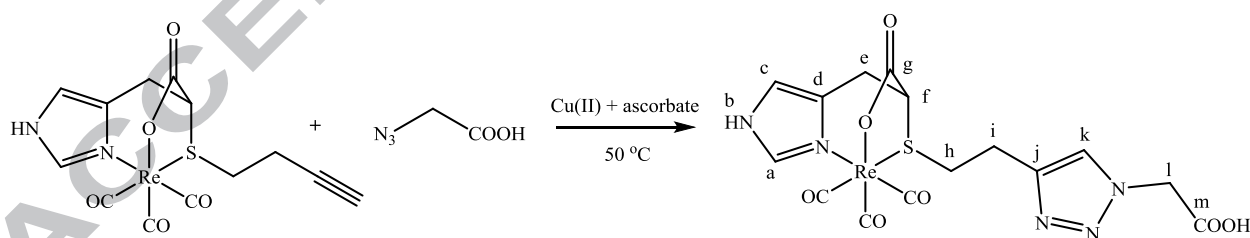
CD<sub>3</sub>OD)  $\delta$ : 8.12 (s, 1H, a), 7.08 (s, 1H, c), 4.39 (dd,  $J = 4.1$  Hz, 1H, f), 3.64 (dd,  $J = 17.5, 4.2$  Hz, 1H, e), 3.39-3.32 (m, 2H, e, h), 3.24-3.14 (m, 1H, h), 2.76 (t,  $J = 6.2$  Hz, 2H, i), 2.52 (t,  $J = 2.5$  Hz, 1H, k). <sup>13</sup>C NMR (125 MHz, CD<sub>3</sub>OD)  $\delta$ : 196.37, 195.23, 194.79 (CO), 181.08 (g), 141.00 (a), 116.03 (c), 133.96 (d), 79.71 (j), 71.26 (k), 46.57 (f), 39.55 (h), 27.32 (e), 17.59 (i). HRMS ( $m/z$ ): (C<sub>13</sub>H<sub>11</sub>N<sub>2</sub>O<sub>5</sub><sup>187</sup>ReS) 495.0018 calc. for [M+H]<sup>+</sup>, 494.9956 found and 986.9936 calc. for [2M+H]<sup>+</sup>, 986.9713 found.

Purified **3** (1 mg, 0.8  $\mu$ mol) was weighed into a 5 mL pear-shaped flask containing a Teflon stir bar. The flask was sealed with a rubber septum and purged with Ar gas for 15 min. In a separate 5 mL crimp vial, a 2 mg/mL solution of Re-**2** dissolved in 75% *t*-BuOH in water was prepared and then purged with Ar gas for 15 min. Using a syringe, 395  $\mu$ L of the Re-**2** solution (0.79 mg, 0.8  $\mu$ mol) was added to the flask containing the peptide and was then stirred under a gentle stream of Ar gas. In a separate tube, an aqueous solution of NaHCO<sub>3</sub> (1.6  $\mu$ mol in 22.5  $\mu$ L H<sub>2</sub>O), ascorbic acid (1.6  $\mu$ mol in 47  $\mu$ L H<sub>2</sub>O), and CuSO<sub>4</sub>·5H<sub>2</sub>O (0.8  $\mu$ mol in 22.5  $\mu$ L H<sub>2</sub>O) was prepared; CuSO<sub>4</sub> was the final reagent added and caused the mixture to quickly become yellow and cloudy. This entire mixture (92  $\mu$ L) was immediately transferred via syringe into the reaction flask along with an additional 100  $\mu$ L of H<sub>2</sub>O rinsate, and the reaction was heated at 50 °C for 3.5 h. Two Re-**4-pre** isomers formed and were purified collectively using analytical HPLC with an isolated yield of 13% (determined by ICP-MS) and were lyophilized and stored at -20 °C. LC-ESI-MS ( $m/z$ ): (C<sub>69</sub>H<sub>78</sub>N<sub>17</sub>O<sub>19</sub><sup>187</sup>ReS<sub>3</sub>) 1732.4 calc. for [M+H]<sup>+</sup>, 1732.4 found and 866.7 calc. for [M+2H]<sup>2+</sup>, 867.0 found.  $t_R$ : 11.5 and 11.8 min (System 3, Method 4).

### 2.8 Synthesis of *fac*-[Re(CO)<sub>3</sub>(2-1-acetic acid-1,2,3-triazole)] (Re-**2-model**)

In a 10 mL round bottom flask, Re-**2** (17 mg, 0.034 mmol) was dissolved in 75% *t*-BuOH in water (2.3 mL). To this, a solution of 2-azidoacetic acid (3  $\mu$ L, 0.04 mmol) in 0.5 mL of water

was added. The flask was sealed with a rubber septum and flushed with a gentle N<sub>2</sub> gas flow for 15 min. In a separate 10 mL vial, ascorbic acid (2.5 mg, 0.014 mmol) was dissolved in 0.5 mL of water, to which was added an aqueous 1 M NaHCO<sub>3</sub> solution (14 μL, 0.014 mmol) and then CuSO<sub>4</sub>·5H<sub>2</sub>O (1.9 mg, 0.007 mmol). After addition of the copper reagent, the solution turned yellow and turbid and was transferred immediately via syringe to the round bottom flask. The reaction was heated at 50 °C for 5 h, at which time the vessel was cooled to room temperature and the *t*-BuOH was removed *in vacuo* to leave behind a white, cloudy precipitate as an aqueous suspension. The suspension was centrifuged, the liquid decanted off, and the precipitate was washed once with water before being fully dried under vacuum to afford 13 mg of **Re-2-model** (64% yield, Scheme 2). IR (KBr, cm<sup>-1</sup>): 2030, 1918, 1903, 1654, 1618. <sup>1</sup>H NMR (500 MHz, CD<sub>3</sub>OD) δ: 8.11 (s, 1H, a), 7.94 (s, 1H, k), 7.06 (s, 1H, c), 5.18 (t, 1H, l), 4.22 (t, J = 4.2 Hz, 1H, f), 3.62 (dd, J = 3.4, 17.5 Hz, 1H, e), 3.48 (dd, J = 7.0, 14.1 Hz, 1H, h), 3.39 (m, 1H, h), 3.32 (m, 1H, e), 3.25 (m, 2H, i). <sup>13</sup>C NMR (125 MHz, CD<sub>3</sub>OD) δ: 162.58 (m), 140.95 (a), 135.15 (j), 134.04 (d), 132.56 (k), 115.98 (c), 54.25 (l), 46.42 (f), 40.27 (h), 27.32 (e), 23.69 (i). HRMS (*m/z*): (C<sub>15</sub>H<sub>14</sub>N<sub>5</sub>O<sub>7</sub><sup>187</sup>ReS) 618.0062 calc. for [M+Na]<sup>+</sup>, 618.0109 found.



Scheme 2. Synthesis of the model complex, **Re-2-model**.

### 2.9 Concentration Determinations for Solutions of 4 and Re-4

ICP-MS analyses were performed for Re-**4-pre**, Re-**4-post**, and **4**, as previously described.<sup>11</sup> The purified and lyophilized Re products were dissolved into a 10% methanol in water solution, while purified and lyophilized **4** was dissolved into a 20% methanol in water solution. All solutions were prepared to a targeted concentration of approximately 1 mg/mL. Briefly, each solution was aliquoted (13-15  $\mu$ L) in duplicate into acid-washed, pre-weighed tubes. The tubes were reweighed and the solutions were digested with 150  $\mu$ L of concentrated HNO<sub>3</sub> and then heated for 1 h at 100 °C. The digestate volume was brought to approximately 5 mL with ultrapure water<sup>1</sup> and then weighed a final time. Afterwards, aliquots were removed for further dilution and fortification with Be/Sc/Y/Tl internal standards of known concentration (undiluted digestate was also analyzed). Internal standards were likewise added to a series of calibration standards prepared from MS-D Multielement Standard stock solutions (High Purity Standards, Charleston, SC), which contained Re and S at ppb levels. Mean results were used, as measured by signals from <sup>32</sup>S for S and both <sup>185</sup>Re and <sup>187</sup>Re for Re. Solvent and digestion blanks were analyzed in similar fashion.

### 2.10 *In Vitro* Receptor Binding Affinity

The binding affinities of Re-**4-pre** and Re-**4-post** for SSTRs in rat pancreatic cancer (AR42J) cells were each determined by competition for binding sites with the radioligand standard [<sup>125</sup>I]iodo-Tyr<sup>11</sup>-somatostatin-14. The AR42J cells were cultured by the Cell and Immunobiology Core at the University of Missouri (Columbia, MO) in RPMI 1640 medium with 4.5 g/L glucose

---

<sup>1</sup> Water was passed through a PURELABR Pulse 1 (ELGA LabWater), producing 15.0 M $\Omega$ .cm water. This water was then passed through a PURELABR Flex 2 UV/TOC (ELGA LabWater), which produced Type I, 18.2 M $\Omega$ .cm water via UV oxidation of organics and ion exchange. The total oxidizable carbon specification (TOC) was <5 ppb.

(GIBCO-Invitrogen, Carlsbad, CA) that was supplemented with 10% fetal bovine serum, 2 mM L-glutamine, and 50  $\mu\text{g}/\text{mL}$  gentamycin. Cells were incubated at 37 °C in a 5%  $\text{CO}_2$  atmosphere and harvested using a soybean trypsin inhibitor.

The competition assay was performed similarly to a previously published method.<sup>11</sup> Serial dilutions in binding buffer (0.25% bovine serum albumin in GIBCO-Invitrogen RPMI 1640 media) were performed to make solutions of Re-4 ranging from  $3 \times 10^{-5}$  M to  $3 \times 10^{-12}$  M (by 10-fold dilution factors). Into 1.5 mL centrifuge tubes were added: 100  $\mu\text{L}$  of Re-4, 100  $\mu\text{L}$  of [ $^{125}\text{I}$ ]iodo-Tyr<sup>11</sup>-somatostatin-14 in binding buffer (100,000 cpm), and 100  $\mu\text{L}$  of AR42J cells ( $2 \times 10^6$  cells, pre-washed twice with binding buffer). Each Re-4 concentration was tested in triplicate, and final concentrations were  $1 \times 10^{-5}$  M to  $1 \times 10^{-12}$  M. Additionally, three replicates contained 100  $\mu\text{L}$  of binding buffer in place of the Re-4 solution, as zero concentration standards. The tubes were incubated for 1 h in a laminar flow hood at room temperature and were manually shaken once every 15 min. After incubation was complete, the cells were handled using cold trays. The cells were centrifuged at 6000 rpm for 30 seconds, and the pellets were washed with refrigerated binding buffer. This was repeated twice more to remove unbound [ $^{125}\text{I}$ ]iodo-Tyr<sup>11</sup>-somatostatin-14. Finally, the supernatant was removed and the pellets were counted on a Multi-Wiper gamma counter (Laboratory Technologies, Inc., Elburn, IL). Data analysis was performed using GraphPad Prism 6 software (La Jolla, CA).

### 2.11 Synthesis of *fac*-[ $^{99\text{m}}\text{Tc}$ ][ $\text{Tc}(\text{CO})_3(\mathbf{4})$ ] ([ $^{99\text{m}}\text{Tc}$ ]Tc-4)

The [ $^{99\text{m}}\text{Tc}$ ]triaquatricarbonyltechnetium (I) precursor, [ $^{99\text{m}}\text{Tc}$ ][ $\text{Tc}(\text{OH})_3(\text{CO})_3$ ]<sup>+</sup>, was synthesized by adding 0.8-1 mL of [ $^{99\text{m}}\text{Tc}$ ][ $\text{TcO}_4$ ]<sup>-</sup> (10-20 mCi, 370-740 MBq) in saline from a  $^{99}\text{Mo}/^{99\text{m}}\text{Tc}$  generator (Mallinckrodt Pharmaceuticals, St. Louis, MO) to a kit prepared in-house

according to a literature procedure.<sup>24</sup> Briefly, a 5 mL crimp vial containing 5.5 mg of NaBH<sub>4</sub>, 4 mg of Na<sub>2</sub>CO<sub>3</sub>, and 10 mg of Na/K tartrate (the kit) was flushed with CO(g) for 15 min immediately prior to addition of [<sup>99m</sup>Tc][TcO<sub>4</sub>]<sup>-</sup>. Subsequent heating at 100 °C for 20 min yielded a solution of [<sup>99m</sup>Tc][Tc(OH)<sub>2</sub>(CO)<sub>3</sub>]<sup>+</sup>, which was then pH adjusted to 6 using 1 M HCl. The precursor formation was verified by HPLC (System 3, Method 4, t<sub>R</sub> = 5 min) with a radiochemical yield (RCY) of ≥ 98%.

To 18 μL of **4** (1.13 mM in an aqueous solution of 20% MeOH), 186 μL of [<sup>99m</sup>Tc][Tc(OH)<sub>2</sub>(CO)<sub>3</sub>]<sup>+</sup> (2-5 mCi, 74-185 MBq) was added to give a final ligand concentration of 1 × 10<sup>-4</sup> M. The solution was heated at 75 °C for 30 min to give a RCY of 65% ± 5% (n=5) for the major [<sup>99m</sup>Tc]Tc-**4** product, which was purified via analytical HPLC (System 3, Method 4, t<sub>R</sub> = 16.1 min).

To concentrate [<sup>99m</sup>Tc]Tc-**4** and remove TFA, the HPLC-collected product fraction was processed through a Waters Sep-Pak C18 Light cartridge that had been preconditioned with 10 mL of absolute ethanol (EtOH) followed by 10 mL of H<sub>2</sub>O. The product fraction was first diluted to 20 mL with high purity 18 MΩ.cm H<sub>2</sub>O and then loaded onto the pre-conditioned Sep-Pak. The Sep-Pak was washed with 10 mL of H<sub>2</sub>O, and the [<sup>99m</sup>Tc]Tc-**4** was eluted with 400 μL of absolute EtOH into a 1.5 mL centrifuge tube containing approximately 1 mg of gentisic acid (GA) as a radioprotectant. The EtOH was evaporated using gentle heating (≈ 55 °C water bath) and a light flow of N<sub>2</sub> gas, and the <sup>99m</sup>Tc-labeled complex was reconstituted in a solution of 1% Tween 80 in 10 mM phosphate-buffered saline (PBS).

### 2.12 In Vitro [<sup>99m</sup>Tc]Tc-**4** Stability Studies

Purified and concentrated product was aliquoted (30 μL) into three 1.5 mL centrifuge tubes along with 30 μL of either 10 mM cysteine or 10 mM histidine in PBS and subsequently diluted with

240  $\mu\text{L}$  of 10 mM PBS. The final solution pH was 7.4, the final amino acid concentration was 1 mM, and the final Tween 80 concentration was 0.1%. In the case of mouse sera studies, 30  $\mu\text{L}$  aliquots of [ $^{99\text{m}}\text{Tc}$ ]Tc-4 were diluted 10-fold using whole mouse sera (Sigma Life Science, St. Louis, MO).

The solutions were incubated at 37  $^{\circ}\text{C}$  and the percentage of intact complex was determined at various time points via HPLC (System 3, Method 4). Small aliquots from the histidine and cysteine solutions were directly injected into the HPLC for analysis at 1 h, 4 h, and 24 h. Larger mouse sera incubation aliquots were taken, diluted with three volumes of MeCN, vortexed and then centrifuged at 2500 rpm for 5 min. The MeCN layer was removed and the protein pellet was washed once with three volumes of MeCN, vortexed, and centrifuged. After separation, the combined MeCN layers and the pellet were each counted on a dose calibrator (Capintec, Ramsey, NJ) to determine the percentage of protein binding. The MeCN supernatant was then concentrated to dryness using a stream of  $\text{N}_2$  gas and gentle heating ( $\approx 55$   $^{\circ}\text{C}$  water bath), reconstituted in 1% Tween 80 in 10 mM PBS, and injected for HPLC analysis.

### 2.13 Distribution Coefficient Determination

A glass test tube was filled with 2 mL of water and 2 mL of *n*-octanol. While vortexing, 50  $\mu\text{L}$  of purified and concentrated [ $^{99\text{m}}\text{Tc}$ ]Tc-4 (approximately 7.4  $\mu\text{Ci}$ , 0.27 MBq) was added to the test tube. Vortexing was continued for 30 additional seconds, and the tube was then centrifuged for 10 min. A 50  $\mu\text{L}$  aliquot was removed from the aqueous (pH 7) and organic layers and counted on a NaI(Tl) well detector. This process was repeated for a total of three replicates. The  $\log D_7$  was calculated using the following equation:  $\log D_7 = \log (\text{cpm}_{\text{oct}}/\text{cpm}_{\text{wat}})$ .

#### 2.14 *In Vivo* Biodistribution and Imaging Studies

All animal studies were conducted in compliance with a protocol approved by the Subcommittee for Animal Studies of the Harry S. Truman Memorial Veterans' Hospital and the Animal Care and Use Committee of the University of Missouri-Columbia Animal Care Quality Assurance Office. Female ICR SCID mice (Taconic, Hudson, NY), age 6 weeks, were inoculated with  $5 \times 10^6$  AR42J cells via subcutaneous injection in the right hind flank. Imaging studies were conducted 2 weeks after inoculation, and biodistribution studies were conducted 2.5 weeks after inoculation.

The mouse dosing solutions were prepared by HPLC purification and Sep-Pak concentration of the [ $^{99m}\text{Tc}$ ]Tc-4 product, as described above, except with reconstitution of the  $^{99m}\text{Tc}$ -labeled product in 0.1% Tween 80 in sterile saline (vs. 1% Tween 80 in PBS). The solution pH was adjusted to neutral with 0.1 M NaOH, and the final volume was adjusted with 0.1% Tween 80 in sterile saline to yield the desired concentration. Finally, the solution was passed through a 0.22  $\mu\text{m}$  sterile nylon filter.

The final activity concentrations for the biodistribution doses were: (1) regular dose, 4.5  $\mu\text{Ci}$  (0.17 MBq) in 100  $\mu\text{L}$  and (2) blocking dose, 4.5  $\mu\text{Ci}$  (0.17 MBq) in 150  $\mu\text{L}$  containing 150  $\mu\text{g}$  of SS-14. Mice ( $n = 4$  for each group) were humanely sacrificed by cervical dislocation at 1 h and 4 h post-injection, and their organs and tissues were collected and then counted on a Wallac 1480 Wizard 3" gamma counter from Perkin Elmer. Mice that received a blocking dose were only evaluated at the 4 h time point.

The final activity concentrations for the imaging doses were: (1) regular dose, 70  $\mu\text{Ci}$  (2.6 MBq) in 100  $\mu\text{L}$  and (2) blocking dose, 70  $\mu\text{Ci}$  (2.6 MBq) in 150  $\mu\text{L}$  containing 150  $\mu\text{g}$  of SS-14. Studies were performed on live mice and microSPECT/CT images were taken at 1 and 4 h post-

injection. Mice were anesthetized using 3% isoflurane at induction and 2.5% isoflurane during imaging. Mice were kept warm during imaging with a heating coil located on the imaging platform. Imaging data were collected using a SIEMENS Inveon MicroSPECT/CT scanner (Siemens Medical Solutions, Malvern, PA). Spiral SPECT imaging was performed using MWB 1.0 mm collimators with a 35 mm radius of rotation and 120 projections. The images were reconstructed using OSEM3D. The CT images were captured using an 80 kVp x-ray source and 360° data acquisition for 3D volume-rendered data. The images were reconstructed in real-time using Fan beam (Feldkamp) filtered back projection algorithms and were processed using Inveon Research Workplace processing software.

### 3 Results and Discussion

#### 3.1 Synthesis of **2** and **4**

Previously, highly stable Re- and  $^{99m}\text{Tc}$ -labeled tricarbonyl complexes were reported using a tripodal [N,S,O] chelation design, where N-imidazole, S-thioether, and O-carboxylate donor atoms participated in the coordination sphere.<sup>25–29</sup> A chelator employing the same chelation strategy (Figure 1C) was thus adopted for **2**. However, in contrast to previous [N,S,O] chelators, **2** was functionalized with an alkyne group (Figure 1B) rather than a carboxylate group, to allow for conjugation to the sst<sub>2</sub>-ANT peptide via an azide-alkyne click reaction.

The synthesis of **2** is depicted in Scheme 1. The reaction of 3-butynol with methane sulfonyl chloride in anhydrous DCM led to the mesylated derivative (**1a**), which was isolated in 90% yield. Reaction of **1a** with cesium thioacetate (generated *in situ*) gave the thiolate derivative (**1b**), which was isolated in 82% yield. As a final step, **1b** and 2-chloro-3-(1H-imidazol-4-yl)propanoic acid were reacted in an aqueous 1 M NaOH solution for 7 days to yield **L**. Due to

the selective nature of Cu(I)-assisted azide-alkyne cycloaddition reactions, the addition of protecting groups to **2** prior to peptide conjugation was not required.

Compound **4** was synthesized using Fmoc SPPS. The sst<sub>2</sub>-ANT peptide was functionalized with an azidoacetyl group at the *N*-terminus to yield linear **3**, to which **2** was conjugated via a Cu(I)-assisted click reaction. After deprotection and cleavage from the resin, LC-ESI-MS analysis of the crude reaction mixture confirmed the formation of the desired disulfide-cyclized L-sst<sub>2</sub>-ANT product, along with cyclized unconjugated **3**.<sup>30</sup> Both the **3** and **4** were successfully purified using semi-preparative HPLC (System 1, Method 1).

### 3.2 Synthesis of Rhenium Complexes

Using a post-complexation synthetic method, the [Re(CO)<sub>3</sub>]<sup>+</sup> complex with **2** was formed after conjugation between **2** and sst<sub>2</sub>-ANT. This mimicked the preferred approach for radiotracer syntheses, in which the radioactive component is incorporated in the final synthetic step in order to minimize loss of radioactivity due to decay, to reduce personnel exposure, etc. Here, the reaction of [Re(OH<sub>2</sub>)<sub>3</sub>(CO)<sub>3</sub>]<sup>+</sup> with **4** yielded two Re-**4-post** isomeric products in a ~1:1 ratio with an 84% reaction yield (determined by HPLC), which were collectively purified by analytical HPLC. The observation of isomers was not surprising, as isomer formation upon coordination of the [Re(CO)<sub>3</sub>]<sup>+</sup> core with the [N,S,O] chelator can be caused by the combination of two factors: the chiral C center of the chelator, yielding enantiomers, and the two coordination orientations that are possible with the prochiral S-donor of the chelator, leading to two diastereomers (each being a pair of enantiomers). The chirality of the sst<sub>2</sub>-ANT peptide further adds to the isomeric products possible. Similar observations were made in our previous work, as well as with other chelators containing chiral C and prochiral S atom donors.<sup>12,20</sup> LC-ESI-MS

and HRMS analyses of Re-**4-post** resulted in an excellent match between the calculated and observed mass-to-charge ratios ( $m/z$ ) and demonstrated the expected isotopic pattern for both the singly- and doubly-charged species.

The click conjugation of the chelator **2** to the peptide sst<sub>2</sub>-ANT results in the formation of a triazole ring, and with it, a possible competing N-triazole ( $N_{tr}$ ) donor atom. The use of triazole rings to provide a nitrogen donor for chelation of  $[M(CO)_3]^+$  ( $M = Re, {}^{99m}Tc$ ) has been described previously.<sup>31</sup> And similar to the N-imidazole ( $N_{im}$ ) donor with its three-carbon distance to the adjacent S-thioether donor,  $N_{tr}$  coordination would also yield a six-membered metal ring to form a neutral  $[N,S,O]$  complex. Thus, while the findings from the post-complexation method were consistent with  $[N,S,O]$  coordination, distinction could not be made between tripodal  $[N_{im},S,O]$  and linear  $[N_{tr},S,O]$  modes (Figure 3A and 3B, respectively). Further possible was the linear  $[N_{tr},S,N_{im}]$  coordination to yield a monocationic Re-**4** complex (Figure 3C). A pre-complexation synthetic route was therefore also explored, wherein the Re-**2** complex with the intended tripodal  $[N_{im},S,O]$  coordination was formed prior to click conjugation, thereby effectively eliminating competition between  $N_{im}$  and  $N_{tr}$  donor atoms for metal coordination.

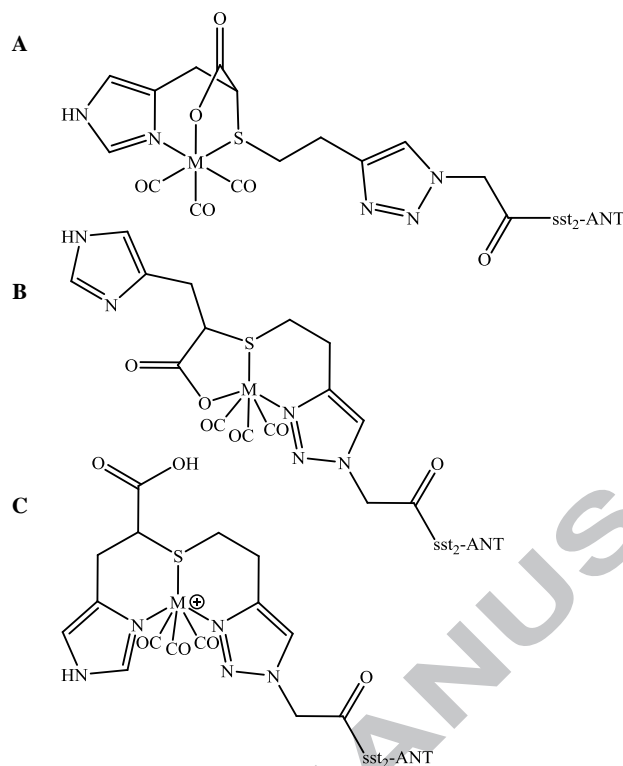


Figure 3. (A) The intended tripodal  $[N_{im},S,O]$  coordination mode of  $fac-[M(CO)_3(\mathbf{4})]$  vs. the alternative (B) linear  $[N_{tr},S,O]$  and (C) linear  $[N_{tr},S,N_{im}]$  coordination modes;  $M = Re, {}^{99m}Tc$ .

The pre-complexation method used a Cu(I)-assisted click reaction of pre-complexed Re-**2** with **3** for synthesizing Re-**4-pre**. Prior to this reaction, the Re-**2** was synthesized, yielding one major product that was purified by semi-preparative HPLC (System 2, Method 3) and subsequently confirmed by NMR to correspond to a single diastereomer. The  $[N_{im},S,O]$  coordination mode of Re-**2** was verified by  ${}^1H$ -NMR and COSY, as well as by comparison against previous complexes bearing the same chelating unit.<sup>25,28,29</sup> The Re-**4-pre** product that was obtained by click conjugation of Re-**2** with the chiral chelator-peptide **3** was also comprised of two isomers, similar to Re-**4-post**. LC-ESI-MS analysis of the Re-**4-pre** products demonstrated the expected isotopic pattern with  $m/z$  that matched the calculated value. However, upon HPLC co-injection of the Re-**4-pre** and Re-**4-post** products, differences in retention times were observed, with the Re-**4-pre** isomers eluting approximately 1.7 min later than the Re-**4-**

**post** isomers ( $t_R = 9.8$  and  $10.2$  min for Re-**4-post** and  $11.5$  and  $11.8$  min for Re-**4-pre**; System 3, Method 4).

To further verify the  $[N_{im},S,O]$  coordination mode of Re-**4-pre**, a model clicked complex was prepared through the reaction of Re-**2** with azidoacetic acid (Scheme 2). The single diastereomer product, Re-**2-model**, was purified by semi-preparative HPLC (System 2, Method 3) and was characterized by IR, NMR and HRMS. The spectroscopic characterization indicated that Re-**2-model** had indeed maintained the original  $[N_{im},S,O]$  coordination through the click conjugation. The NMR pattern of the protons that participate in the chelating unit matched those of Re-**2**. In particular, the imidazole shifts were very similar, indicating that the imidazole was coordinated with the metal in both complexes. Furthermore, the shifts of the H-e protons were in the same range [3.64 (dd,  $J = 17.5, 4.2$  Hz), 3.39-3.32 (m) for Re-**2** and 3.62 (dd,  $J = 17.5, 3.4$  Hz), 3.32 (m) for Re-**2-model**], and the H-i protons appeared as a multiplet, consistent with a pendant moiety. Conversion to the linear coordination mode  $[N_{tr},S,N_{im}]$  would result in different H-e proton shifts.<sup>25</sup> It would also result in the splitting of the two H-i protons into two sets of peaks, as is common for the methylene protons participating in a chelator's backbone, but not observed here. Therefore, the Re-**4-pre** product is well-supported to involve the tripodal  $[N_{im},S,O]$  coordination of the Re-tricarbonyl core by **4** (Figure 3A).

The exact nature of Re-**4-post** remains unclear. While the observed difference in HPLC retention times might be explained by  $[N_{im},S,O]$  coordination with slightly different conformational preferences due to the additional steric bulk of the peptide-conjugated ligand, perhaps more likely is that Re-**4-post** adopted an alternate binding mode, such as with neutral linear  $[N_{tr},S,O]$  coordination (Figure 3B) or with monocationic linear  $[N_{tr},S,N_{im}]$  coordination (Figure 3C). However, spectroscopic data to support which binding mode is present in Re-**4-post**

were not obtained due to the fact that our efforts to synthesize the model clicked chelator (via conjugation of **2** with azidoacetic acid) were unsuccessful.

### 3.3 *In Vitro* Receptor-Binding Affinity

The SSTR binding affinity of Re-**4** was determined for both the Re-**4-pre** and Re-**4-post** products by a competitive binding assay in SSTR2-expressing rat pancreatic cancer (AR42J) cells. Low nanomolar affinity was retained by sst<sub>2</sub>-ANT after its *N*-terminal modification, regardless of the reaction pathway used to synthesize Re-**4**. The IC<sub>50</sub> values of 27 ± 13 nM (Re-**4-post**) and 19 ± 14 nM (Re-**4-pre**) shown in Figure 4 are comparable to that of our previously reported bioconjugate complex [Re(CO)<sub>3</sub>(NSN-sst<sub>2</sub>-ANT)]<sup>+</sup> (15 ± 4 nM).<sup>11</sup> These promising results warranted our further investigation into the preparation of the <sup>99m</sup>Tc analogue, along with its stability and biological evaluations.

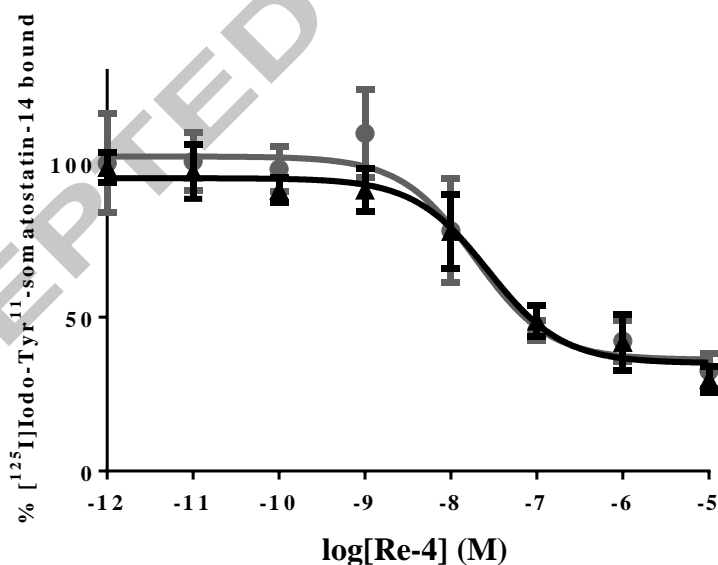


Figure 4. Binding affinities for Re-**4-pre** (grey) and Re-**4-post** (black) in SSTR2-expressing AR42J cells.

### 3.4 Synthesis of [<sup>99m</sup>Tc]Tc-4

The post-conjugation labeling approach (i.e., incorporation of the radiotracer in the final step) was selected for practical reasons, as it is the more advantageous route from the radiosynthetic standpoint, especially for short-lived radioisotopes. The [<sup>99m</sup>Tc][Tc(OH)<sub>2</sub>(CO)<sub>3</sub>]<sup>+</sup> precursor was synthesized using a kit prepared in-house according to a literature procedure.<sup>24</sup> The optimized conditions for synthesizing [<sup>99m</sup>Tc]Tc-4 were found to be adjustment of the precursor solution pH to 6 prior to heating with a solution of **4** at 75 °C for 30 min, with product isolation by HPLC.

Initial <sup>99m</sup>Tc labeling attempts were performed similarly to our previous NSN-sst<sub>2</sub>-ANT labeling (75 °C, 30 min).<sup>11</sup> Heating in the pH range of 5-8 led to four radiolabeled products, all of which exhibited very different HPLC retention times from the Re-**4-pre/post** standards; one early-eluting (*t<sub>R</sub>* = 9.3 min) and three late-eluting (*t<sub>R</sub>* = 16.1 min, 17.6 min, 18.2 min) products were observed with System 3, Method 4. An initial stability measurement of the HPLC-isolated early-eluting product and late-eluting products in 10 mM PBS for 4 h at 37 °C eliminated the early-eluting product from further consideration, as 90% had either oxidized to [<sup>99m</sup>Tc][TcO<sub>4</sub>]<sup>-</sup> or had converted into the late-eluting products. This indicated that the early-eluting isomer was not thermodynamically favored, suggestive of incomplete bidentate coordination.

Attempts to synthetically favor the dominant late-eluting product (*t<sub>R</sub>* = 16.1 min) over the others revealed that the relative product RCYs depended greatly on both the reaction pH and temperature. For example, reactions performed at pH 2 favored the early-eluting product, regardless of the reaction temperature. Only the early-eluting product was formed when the reaction was performed at pH 5 and room temperature (50% RCY, with the remaining activity as the unreacted [<sup>99m</sup>Tc][Tc(OH)<sub>2</sub>(CO)<sub>3</sub>]<sup>+</sup> precursor). However, conversion to the late-eluting

products occurred upon heating, with only 9% of the original early-eluting product remaining. Reaction conditions of pH 6-7 and heating for 30 min at 75 °C gave the highest observed RCY (average 65%) for the dominant late-eluting product, hereafter referred to simply as [ $^{99m}\text{Tc}$ ]Tc-4. All subsequent labeling reactions were therefore performed at a pH of 6, in order to favor formation of this product, which was purified for use in the remaining *in vitro* and *in vivo* studies.

The observation of distinctly different products from the post-conjugation labeling approach with Re and  $^{99m}\text{Tc}$  was initially unexpected; Re and Tc are well known to typically demonstrate similar chemical behaviors, and we had not observed such differences in our earlier work. However, it appears that the [ $^{99m}\text{Tc}$ ]Tc-4 product does not involve the intended [ $\text{N}_{\text{im}},\text{S},\text{O}$ ] coordination mode (Figure 3A). The above findings are consistent with, though not definitive for, a [ $^{99m}\text{Tc}$ ]Tc-4 product with a [ $\text{N}_{\text{tr}},\text{S},\text{O}$ ] or [ $\text{N}_{\text{tr}},\text{S},\text{N}_{\text{im}}$ ] linear coordination mode (Figures 3B or 3C, respectively). The relative hardness of Tc compared to the softer Re may have resulted in a preference for [ $\text{N}_{\text{tr}},\text{S},\text{O}$ ] coordination.

### 3.5 In Vitro Stability Studies

After HPLC purification, the [ $^{99m}\text{Tc}$ ]Tc-4 product was concentrated using a Sep-Pak C-18 Light cartridge, from which it was eluted in absolute EtOH into a vial containing gentisic acid as a radioprotectant. The EtOH was removed and the product was reconstituted in 1% Tween 80 in 10 mM PBS for use in stability studies. This [ $^{99m}\text{Tc}$ ]Tc-4 solution was aliquoted to new tubes and diluted 10-fold with either cysteine or histidine (1 mM final concentrations), or with whole mouse sera. The percentage of intact complex was monitored by HPLC at 1, 4, and 24 h.

The [ $^{99m}\text{Tc}$ ]Tc-4 product demonstrated excellent stability in both the cysteine and histidine challenge studies, with at least 98% of the complex intact through 24 h (Table 1). In the mouse sera studies, carried out through 4 h, the majority of the radioactivity remained in the supernatant (73% at 4 h), demonstrating moderately low protein binding. HPLC analysis of the supernatant radioactivity showed that the large majority of the complex was intact (75% intact at 4 h). The remainder of the radioactivity existed as an unknown degradation product (System 3, Method 4,  $t_R = 13.1$  min), possibly a small protein adduct, but clearly not [ $^{99m}\text{Tc}$ ][ $\text{TcO}_4^-$ ] ( $t_R = 2.7$  min).

Table 1. *In vitro* stability<sup>a</sup> of [ $^{99m}\text{Tc}$ ]Tc-4

	1 h	4 h	24 h
Cysteine	100 ± 0	100 ± 0	100 ± 0
Histidine	98 ± 2	99.7 ± 0.5	99.7 ± 0.5
Mouse Serum	66 ± 1	75 ± 1	NP

<sup>a</sup> Average percentage ± SD of intact complex relative to percent intact complex at 0 h, n = 3; NP = Not performed

### 3.6 Distribution Coefficient Measurement

The distribution coefficient for [ $^{99m}\text{Tc}$ ]Tc-4 was found by measuring its distribution between *n*-octanol and water. The log  $D_7$  value of -0.44 indicates a fairly even distribution between the water and octanol layers, with the complex being only slightly hydrophilic.

### 3.7 *In Vivo* Biodistribution and Imaging Studies

Female ICR SCID mice were inoculated with  $5 \times 10^6$  AR42J cells in the right hind flank, and tumors were allowed to grow for 2-2.5 weeks. Purified and concentrated [ $^{99m}\text{Tc}$ ]Tc-4 was reconstituted with 0.1% Tween 80 in sterile saline to the desired dosing concentration, and the

pH was adjusted to neutral with 0.1 M NaOH. Blocking doses contained SS-14, the native SSTR ligand, to saturate tumor receptors. MicroSPECT/CT images were captured at 1 h, 1 h block, 4 h, and 4 h block. Biodistribution data were collected at 1 h, 4 h, and 4 h block.

The biodistribution data are presented in Table 2. Tumor uptake was high at 1 h with 4.9 %ID/g, decreasing to 1.6 %ID/g by 4 h. No statistical difference was observed for tumor uptake between the 4 h and 4 h blocking (1.4 %ID/g) time points. Further, the amount of radioactivity measured in the tumor at 4 h was roughly equal to that of the blood pool. These findings indicate that tumor uptake occurred via passive diffusion and non-specific binding rather than by receptor mediation, presumably due to a loss in SSTR affinity associated with the different coordination mode in [<sup>99m</sup>Tc]Tc-4 as compared with the SSTR-targeting Re products. Hepatobiliary clearance was the primary mode of excretion, as seen by high uptake in the small intestine uptake at 1 h (31 %ID/g) that shifted to the large intestine by 4 h (67 %ID/g). Secondary to the intestinal activity, the bulk of the remaining activity at both time points was distributed between the kidney (some renal clearance) and liver. For both kidney and liver, the uptake at 4 h was roughly half that observed at 1 h. Overall, [<sup>99m</sup>Tc]Tc-4 demonstrated significantly faster and more complete clearance compared to the previously studied [<sup>99m</sup>Tc][Tc(CO)<sub>3</sub>(NSN-sst<sub>2</sub>-ANT)]<sup>+</sup>.<sup>11</sup>

Table 2. Biodistribution of [<sup>99m</sup>Tc]Tc-4 in AR42J tumor-bearing mice<sup>a</sup>

Organ	1 h	4 h	4 h blocking <sup>b</sup>
Blood	1.4 ± 0.1	1 ± 1	0.7 ± 0.2
Lung	4.4 ± 0.2	1.6 ± 0.5	3.0 ± 0.2
Liver	22 ± 3	13 ± 3	16 ± 3
Spleen	0.8 ± 0.1	0.3 ± 0.1	0.51 ± 0.09
Stomach	1.0 ± 0.3	1 ± 1 <sup>c</sup>	0.7 ± 0.5
L Int	0.5 ± 0.4	67 ± 8	55 ± 3
Sm Int	31 ± 2	7 ± 1	8 ± 2
Kidney	10.8 ± 0.6	6.0 ± 0.5	6 ± 1
Muscle	0.13 ± 0.04	0.04 ± 0.06	0.01 ± 0.02
Adrenals	0.08 ± 0.05	0.0 ± 0.1	0.3 ± 0.5
Fat	0.03 ± 0.2	0.00 ± 0.00	0.00 ± 0.00
Brain	0.03 ± 0.00	0.00 ± 0.00	0.00 ± 0.00
Pancreas	1.0 ± 0.2	0.2 ± 0.1	0.3 ± 0.3
Tumor	4.9 ± 0.6	1.6 ± 0.3	1.4 ± 0.2

<sup>a</sup> Values reported are mean %ID/g ± SD; n = 4

<sup>b</sup> Co-administration of a 150 µg SS-14 blocking dose

<sup>c</sup> n = 3, Q-test was used to remove outlier with 90% probability

The microSPECT/CT images in Figure 5 support the biodistribution data. Radioactivity was distributed throughout the small intestine at 1 h, with a clear increase in large intestine uptake by 4 h. Tumor uptake was observed in the 1 h image, yet the tumor could not be delineated in the 4 h and 4 h block images. Oxidative decomposition of [<sup>99m</sup>Tc]Tc-4 to [<sup>99m</sup>Tc][TcO<sub>4</sub>]<sup>-</sup> was neither suggested by the *in vitro* studies nor by the *in vivo* biodistribution and imaging data, as uptake in the stomach was very low. While the *in vitro* sera stability study showed an unknown degradation product, it is unlikely that the small amount of degradation observed prevented SSTR binding by the remaining intact complex. It is more likely that the unexpected coordination mode in [<sup>99m</sup>Tc]Tc-4 disrupted the receptor-targeting ability of the peptide.

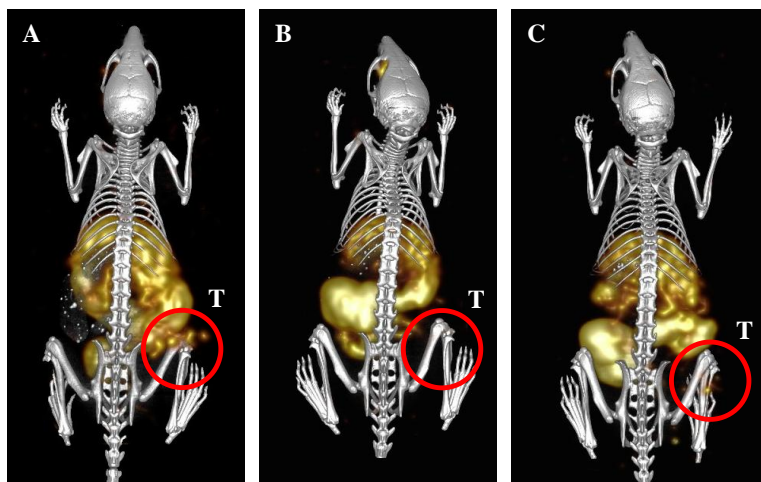


Figure 5. MicroSPECT/CT images of AR42J tumor-bearing mice at (A) 1 h and (B) 4 h post-injection of  $[^{99m}\text{Tc}]\text{Tc-4}$  and (C) at 4 h post-injection with co-administration of a SS-14 blocking dose; tumor location (T).

#### 4 Conclusions

These studies revealed complex chemistry for the labeling of **4** with  $[\text{M}(\text{CO})_3]^+$  ( $\text{M} = \text{Re}, ^{99m}\text{Tc}$ ). The mode of coordination in the Re-**4** product depended upon the synthetic approach used, with the intended neutral tridentate  $[\text{N}_{\text{im}}, \text{S}, \text{O}]$  coordination to the novel bifunctional chelator resulting when the Re tricarbonyl core was complexed by **2** prior to conjugation of the peptide (pre-complexation approach). Both the pre- and post-complexation Re-**4** products exhibited nanomolar *in vitro* SSTR affinity. However, as one of the few instances in which Re and Tc chemistries diverge, the  $^{99m}\text{Tc}$  radiotracer synthesis yielded products different from both of the Re-**4** products. Nonetheless, the dominant  $[^{99m}\text{Tc}]\text{Tc-4}$  product was isolated and shown to exhibit excellent *in vitro* stability. An improvement in *in vivo* clearance was also observed for  $[^{99m}\text{Tc}]\text{Tc-4}$  in comparison to our previously evaluated  $^{99m}\text{Tc}$ -labeled SSTR2-antagonist,  $[^{99m}\text{Tc}][\text{Tc}(\text{CO})_3(\text{NSN-sst}_2\text{-ANT})]^+$ ; however, the new binding mode resulted in a loss of SSTR affinity. Future studies with small model  $[\text{N}, \text{S}, \text{O}]$  chelator complexes of  $^{99g}\text{Tc}$  may provide a better understanding of how the Tc and Re coordination modes differ, and may ultimately allow

for structural confirmation of the [ $^{99m}\text{Tc}$ ]Tc-4 product. Additionally, a longer spacer between the thioether sulfur and alkyne components of the [N,S,O] chelator, to increase the metal ring size formed by coordination of the triazole nitrogen and disfavor its involvement in the complex, may yield a  $^{99m}\text{Tc}$ -labeled product with the intended tripodal [ $\text{N}_{\text{im}},\text{S},\text{O}$ ] coordination mode and realign the Re and Tc product structures.

Acknowledgments: We gratefully acknowledge the support provided by the VA Biomolecular Imaging Center at the Harry S. Truman VA Hospital and the University of Missouri. We thank the Department of Veterans Affairs for providing resources and use of facilities at the Truman VA Hospital. We also thank the following individuals for their technical expertise and contributions: Jim Guthrie (ICP-MS), Kathy Schreiber and Susan Rottinghaus (cell culture), and Mark Lee (HRMS).

Funding: This work was supported by the University of Missouri Research Board [grant number RB 14-08], the Department of Energy Heavy Elements Program [grant number DE-FG02-09ER16097], and the National Science Foundation IGERT [grant number DGE-0965983].

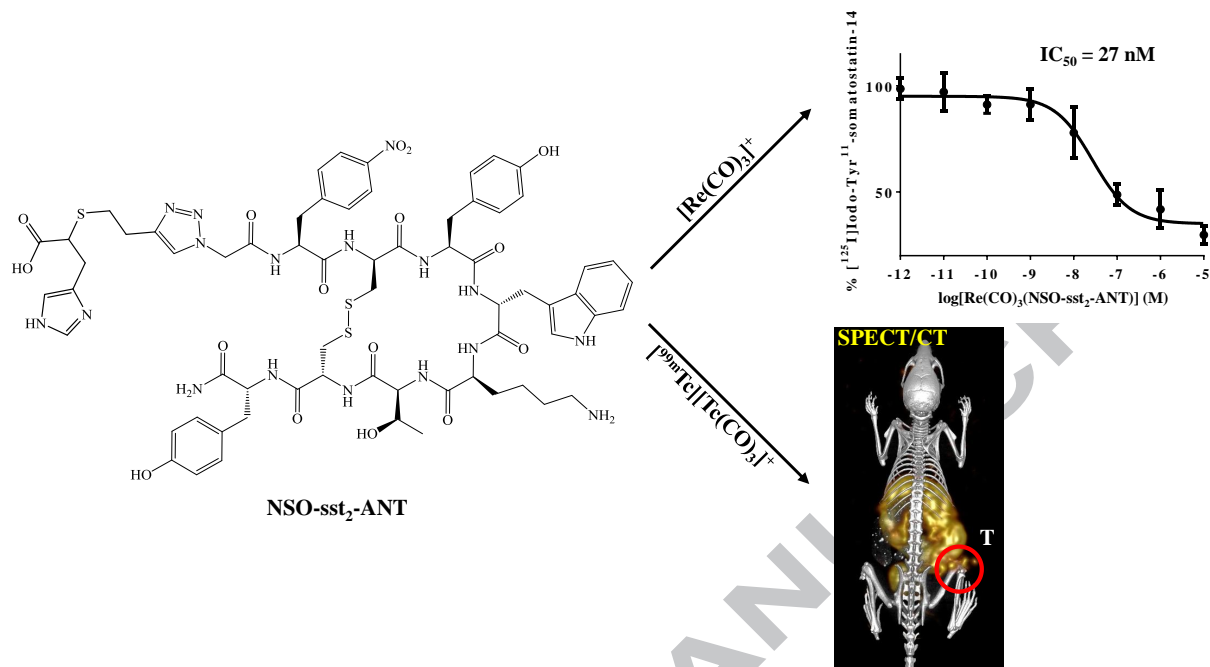
1. Ginj M, Zhang H, Waser B, et al. Radiolabeled somatostatin receptor antagonists are preferable to agonists for *in vivo* peptide receptor targeting of tumors. *Proc Natl Acad Sci.* 2006;103(44):16436-16441. doi:10.1073/pnas.0607761103
2. Bass RT, Buckwalter BL, Patel BP, et al. Identification and characterization of novel somatostatin antagonists. *Mol Pharmacol.* 1996;50(4):709-715.
3. Cescato R, Erchegyi J, Waser B, et al. Design and *in vitro* characterization of highly sst2-selective somatostatin antagonists suitable for radiotargeting. *J Med Chem.* 2008;51(13):4030-4037. doi:10.1021/jm701618q

4. Wild D, Fani M, Fischer R, et al. Comparison of somatostatin receptor agonist and antagonist for peptide receptor radionuclide therapy: A pilot study. *J Nucl Med.* 2014;55(8):1248-1252.
5. Abiraj K, Mansi R, Tamma M-L, et al. Bombesin antagonist-based radioligands for translational nuclear imaging of gastrin-releasing peptide receptor-positive tumors. *J Nucl Med.* 2011;52(12):1970-1978. doi:10.2967/jnumed.111.094375
6. Kim K, Zhang H, Rosa SL, et al. Bombesin antagonist-based radiotherapy of prostate cancer combined with WST-11 vascular targeted photodynamic therapy. *Clin Cancer Res.* 2017;23(13):3343-3351. doi:10.1158/1078-0432.CCR-16-2745
7. Mikaeili A, Erfani M, Sabzevari O. Synthesis and evaluation of a  $^{99m}\text{Tc}$ -labeled chemokine receptor antagonist peptide for imaging of chemokine receptor expressing tumors. *Nucl Med Biol.* 2017;54:10-17. doi:10.1016/j.nucmedbio.2017.07.004
8. Hubalewska-Dydejczyk A, Szybinski P, Trofimiuk M, et al. Expression of the somatostatin receptors (SSTRs) in patients with gastro-pancreatic neuroendocrine tumours (GEP-NET) and medullary thyroid cancers (MTC). May 2008. <http://www.endocrine-abstracts.org/ea/0016/ea0016p294.htm>. Accessed 25 June 2018.
9. Kukwa W, Andrysiak R, Kukwa A, et al.  $^{99m}\text{Tc}$ -octreotide scintigraphy and somatostatin receptor subtype expression in juvenile nasopharyngeal angiofibromas. *Head Neck.* 2011;33(12):1739-1746. doi:10.1002/hed.21668
10. Wild D, Fani M, Behe M, et al. First clinical evidence that imaging with somatostatin receptor antagonists is feasible. *J Nucl Med.* 2011;52(9):1412-1417.
11. Radford L, Gallazzi F, Watkinson L, et al. Synthesis and evaluation of a  $^{99m}\text{Tc}$  tricarbonyl-labeled somatostatin receptor-targeting antagonist peptide for imaging of neuroendocrine tumors. *Nucl Med Biol.* 2017;47:4-9. doi:10.1016/j.nucmedbio.2016.12.002
12. Makris G, Radford L, Gallazzi F, Jurisson S, Hennkens H, Papagiannopoulou D. Synthesis and evaluation of *fac*- $^{99m}\text{Tc}/\text{Re}(\text{CO})_3^+$  complexes with a new (N,S,N) bifunctional chelating agent: The first example of a *fac*- $[\text{Re}(\text{CO})_3(\text{N,S,N-sst}_2\text{-ANT})]$  complex bearing a somatostatin receptor antagonist peptide. *J Organomet Chem.* 2016;805:100-107.
13. Fani M, Pozzo LD, Abiraj K, et al. PET of somatostatin receptor-positive tumors using  $^{64}\text{Cu}$ - and  $^{68}\text{Ga}$ -somatostatin antagonists: The chelate makes the difference. *J Nucl Med.* 2011;52(7):1110-1118.
14. Lane SR, Nanda P, Rold TL, et al. Optimization, biological evaluation and microPET imaging of copper-64-labeled bombesin agonists,  $^{64}\text{Cu}\text{-NO}_2\text{A-(X)-BBN(7-14)NH}_2$ , in a prostate tumor xenografted mouse model. *Nucl Med Biol.* 2010;37(7):751-761. doi:10.1016/j.nucmedbio.2010.04.016

15. Nanda PK, Pandey U, Bottenus BN, et al. Bombesin analogues for gastrin-releasing peptide receptor imaging. *Nucl Med Biol.* 2012;39(4):461-471. doi:10.1016/j.nucmedbio.2011.10.009
16. Nedrow JR, White AG, Modi J, Nguyen K, Chang AJ, Anderson CJ. Positron emission tomographic imaging of copper 64- and gallium 68-labeled chelator conjugates of the somatostatin agonist Tyr<sup>3</sup>-octreotate. *Mol Imaging.* 2014;13:1-13. doi.org/10.2310/7290.2014.00020
17. Lin M, Welch MJ, Lapi SE. Effects of chelator modifications on <sup>68</sup>Ga-labeled [Tyr<sup>3</sup>]octreotide conjugates. *Mol Imaging Biol MIB Off Publ Acad Mol Imaging.* 2013;15(5):606-613. doi:10.1007/s11307-013-0627-x
18. Schibli R, La Bella R, Alberto R, et al. Influence of the denticity of ligand systems on the *in vitro* and *in vivo* behavior of <sup>99m</sup>Tc(I)-tricarbonyl complexes: A hint for the future functionalization of biomolecules. *Bioconjug Chem.* 2000;11(3):345-351. doi:10.1021/bc990127h
19. García Garayoa E, Schweinsberg C, Maes V, et al. Influence of the molecular charge on the biodistribution of bombesin analogues labeled with the [<sup>99m</sup>Tc(CO)<sub>3</sub>]-core. *Bioconjug Chem.* 2008;19(12):2409-2416. doi:10.1021/bc800262m
20. van Staveren DR, Benny PD, Waibel R, Kurz P, Pak J-K, Alberto R. S-Functionalized cysteine: Powerful ligands for the labelling of bioactive molecules with triaquatricarbonyltechnetium-99m(1+) ([<sup>99m</sup>Tc(OH<sub>2</sub>)<sub>3</sub>(CO)<sub>3</sub>]<sup>+</sup>). *Helv Chim Acta.* 2005;88(3):447-460. doi:10.1002/hlca.200590029
21. Karagiorgou O, Patsis G, Pelecanou M, et al. (S)-(2-(2'-Pyridyl)ethyl)cysteamine and (S)-(2-(2'-pyridyl)ethyl)-*d,l*-homocysteine as ligands for the "fac-[M(CO)<sub>3</sub>]<sup>+</sup>" (M = Re, <sup>99m</sup>Tc) core. *Inorg Chem.* 2005;44(12):4118-4120. doi:10.1021/ic050254r
22. Cheung FK, Hayes AM, Morris DJ, Wills M. The use of a [4 + 2] cycloaddition reaction for the preparation of a series of 'tethered' Ru(II)-diamine and aminoalcohol complexes. *Org Biomol Chem.* 2007;5(7):1093-1103. doi:10.1039/B700744B
23. Abram U, Abram S, Alberto R, Schibli R. Ligand exchange reactions starting from [Re(CO)<sub>3</sub>Br<sub>3</sub>]<sup>2-</sup>. Synthesis, characterization and structures of rhenium(I) tricarbonyl complexes with thiourea and thiourea derivatives. *Inorganica Chim Acta.* 1996;248(2):193-202. doi:10.1016/0020-1693(96)05014-1
24. Alberto R, Schibli R, Egli A, Schubiger AP. A novel organometallic aqua complex of technetium for the labeling of biomolecules: Synthesis of [<sup>99m</sup>Tc(OH<sub>2</sub>)<sub>3</sub>(CO)<sub>3</sub>]<sup>+</sup> from [<sup>99m</sup>TcO<sub>4</sub>]<sup>-</sup> in aqueous solution and its reaction with a bifunctional ligand. *J Am Chem Soc.* 1998;120:7987-7988.
25. Makris G, Karagiorgou O, Papagiannopoulou D, et al. Rhenium(I) and technetium(I) tricarbonyl complexes with [NSO]-type chelators: Synthesis, structural characterization,

- and radiochemistry. *Eur J Inorg Chem.* 2012;2012(19):3132-3139.  
doi:10.1002/ejic.201200056
26. Papagiannopoulou D, Makris G, Tsoukalas C, et al. Rhenium(I) and technetium(I) *fac*-M(NSO)(CO)<sub>3</sub> (M = Re, <sup>99m</sup>Tc) tricarbonyl complexes, with a tridentate NSO bifunctional agent: Synthesis, structural characterization, and radiochemistry. *Polyhedron.* 2010;29(2):876-880. doi:10.1016/j.poly.2009.10.009
27. Papagiannopoulou D, Tsoukalas C, Makris G, et al. Histidine derivatives as tridentate chelators for the *fac*-[M<sup>I</sup>(CO)<sub>3</sub>] (Re, <sup>99m</sup>Tc, <sup>188</sup>Re) core: Synthesis, structural characterization, radiochemistry and stability. *Inorganica Chim Acta.* 2011;378(1):333-337. doi:10.1016/j.ica.2011.08.062
28. Makris G, Tseligka ED, Pirmettis I, Papadopoulos MS, Vizirianakis IS, Papagiannopoulou D. Development and pharmacological evaluation of new bone-targeted <sup>99m</sup>Tc-radiolabeled bisphosphonates. *Mol Pharm.* 2016;13(7):2301-2317. doi:10.1021/acs.molpharmaceut.6b00081
29. Makris G, Papagiannopoulou D. Synthesis, characterization, and biological evaluation of new biotinylated <sup>99m</sup>Tc/Re-tricarbonyl complexes. *J Label Compd Radiopharm.* 2016;59(3):95-102. doi:10.1002/jlcr.3372
30. Abe A, Sasaki T. Sulfhydryl groups in glycolipid transfer protein: Formation of an intramolecular disulfide bond and oligomers by Cu<sup>2+</sup>-catalyzed oxidation. *Biochim Biophys Acta BBA - Biomembr.* 1989;985(1):38-44. doi:10.1016/0005-2736(89)90100-4
31. Kluba CA, Mindt TL. Click-to-chelate: Development of technetium and rhenium-tricarbonyl labeled radiopharmaceuticals. *Molecules.* 2013;18(3):3206-3226. doi:10.3390/molecules18033206

## Graphical Abstract



ACCEPTED MANUSCRIPT